Other calculations show that the vacuum-tube launcher will provide an increase of 10% to 20% in altitude, with a simultaneous decrease of 35–60% in wind effect is obtained.

References

[1] Kumar, S. and Shieh, S. C., "Vacuum-Air Tube System for Low Altitude Meteorological Probes," Project Mountainwell Interim Report 7, July 1968, U.S. Army Research Office—Durham, Durham, N.C.

[2] Kumar, S., Rajan, J. R. N., and Murray, J. J., "Vacuum-Air Missile Boost System," *Journal of Spacecraft and Rockets*, Vol. 1, No. 5, Sept.-Oct. 1964, pp. 464–470.

[3] Lee, E. E., "Further Studies of the Vacuum-Air Missile Boost System," M. S. thesis, 1964, Duke Univ., Durham, N.C.

Solar Array Degradation due to Meteoroid Impacts during Extended Planetary Missions

A. J. Richardson* and J. W. Warren*
North American Rockwell Corporation, Space Division, Downey, Calif.

Nomenclature

A_{L1}, A_{L2} = total area lost due to particle impacts by front or rear surface, m²
A_{L1}', A_{L2}' = area lost per impact by front or rear surface, m²
A_{sp} = solar cell area of the solar array, m²
A_{spe} = effective solar cell area of the solar array, m²
C_1, C_2 = meteoroid flux constants
D_{fz} = fracture zone diameter, cm
d_p = meteoroid particle diameter, cm
$f(R)$ = meteoroid flux spatial distribution function
H_s = substrate hardness, Brinell
K, K_s = penetration equation constants (0.64 and 1.38, respectively)
m = meteoroid particle mass, g
n = number of particle impacts
N = meteoroid flux, impacts/m²-sec
P = total penetration depth, cm
P_r = probability of a particle impact
P_{sc} = penetration into solar cell from rear, cm
P_s = penetration into substrate, cm
t_s = substrate thickness, cm
t_3 = thickness of a glass substrate equivalent to the actual substrate, cm
T_a = mission duration, sec
T_R = effective exposure time, sec
V = particle impact velocity, km/sec
α = ratio of fracture zone diameter to penetration depth in glass (20.0)
ρ = meteoroid particle density, g/cm³
ρ_s = substrate density, g/cm³

Introduction

VERY little degradation has occurred in near-Earth solar array applications, but an asteroid belt or other deep space mission may pose a major problem. Because of current interest in the use of solar electric spacecraft with large solar arrays for future interplanetary scientific investigations it is necessary to define the meteoroid hazard for them. The problem is not the puncture damage caused by chance encounter with a single large meteoroid, but the errosive type damage caused by continually impacting micrometeoroids. Evaluation of this problem requires adoption of a mechanism to describe the solar cell power reduction associated with individual particle impacts, followed by treatment of factors that determine the number of impacts.

Presented as Paper 70-1139 at the AIAA 8th Electric Propulsion Conference, Stanford, Calif., August 31–September 2, 1970; submitted October 6, 1970; revision received January 27, 1971. The work described in this paper was performed for the California Institute of Technology, Jet Propulsion Laboratory under Contract NAS7-100.

* Staff Engineer, Structural Systems and Mechanisms Department.

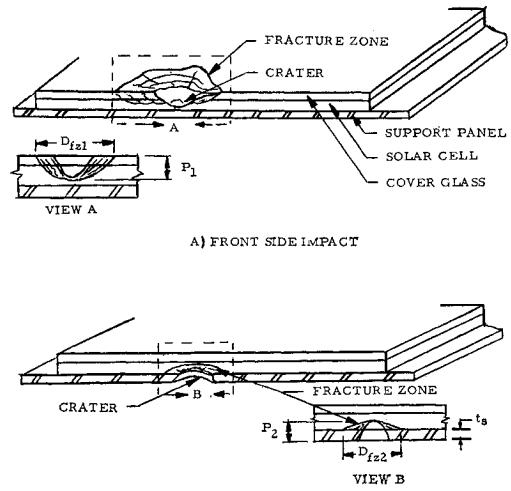

Fig. 1 Solar cell damage modes as a result of micrometeoroized impacts.

Power Loss due to Particle Impact

The results of experimenters, particularly Bowman,[1] provide data on the solar cell power loss resulting from cumulative hypervelocity impacts. However, a method was needed which would account for the difference between laboratory particles and meteoroid particles, i.e., velocity, size, and density. Hypervelocity impacts on glass produce a crater, surrounded by a large fracture zone.[2] These fracture zones will reduce solar cell output by restricting light energy reaching the solar cell rear surface. Figure 1 represents the fracture zone formed by meteoroid impacts on both the front and rear side of the solar panel, and it was assumed that particles impacting the rear side must perforate the substrate before damaging the solar cell. It was also necessary to establish the amount of light reflected by each fracture zone. Evaluating the damaged test articles from the standpoint of optical mechanics, it was concluded that even damage to solar cells by extremely small micrometeoroid particles would produce back-scattering of light. Because of the complex nature of the fissures formed in the damage area, available theoretical methods were judged to be inadequate to establish the exact

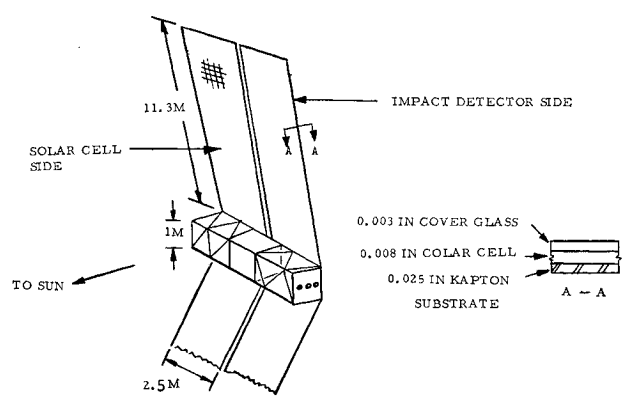

Fig. 2 Spacecraft configuration.

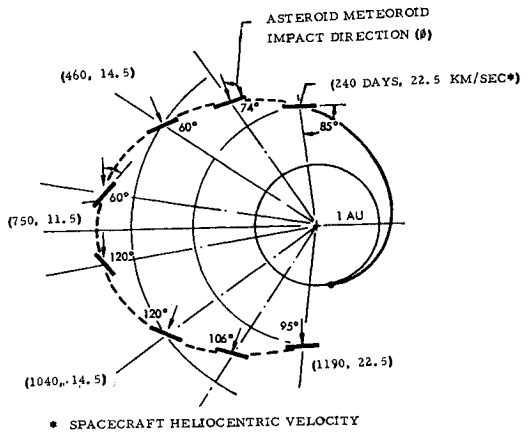

Fig. 3 Study mission and spacecraft orientation.

amount of back-scattering; however, it was estimated that 50% would be the upper limit. A description of the development of the equations used in the analysis follows.

Front surface impacts

The depth of a crater formed in glass by a hypervelocity particle impact is[3]

$$P = K\rho^{1/2}V^{2/3}d_p^{1.2} \tag{1}$$

The fracture zone diameter is $D_{fz} = \alpha P$ and the area loss per impact is

$$A_{L1}' = \pi D_{fz}^2/4 = 0.785\alpha^2(K\rho^{1/2}V^{2/3}d_p^{1.2})^2$$
$$= 1.32\,\alpha^2K^2\rho^{0.2}V^{4/3}m^{0.8} \tag{2}$$

This loss is applicable to the case in which the particle does not perforate the solar cell. Equation (2) is sufficiently accurate for determination of area loss for the perforating meteoroids as well.

The meteoroid population of our solar system is defined in terms of sporadic cometary particles, sporadic asteroidal

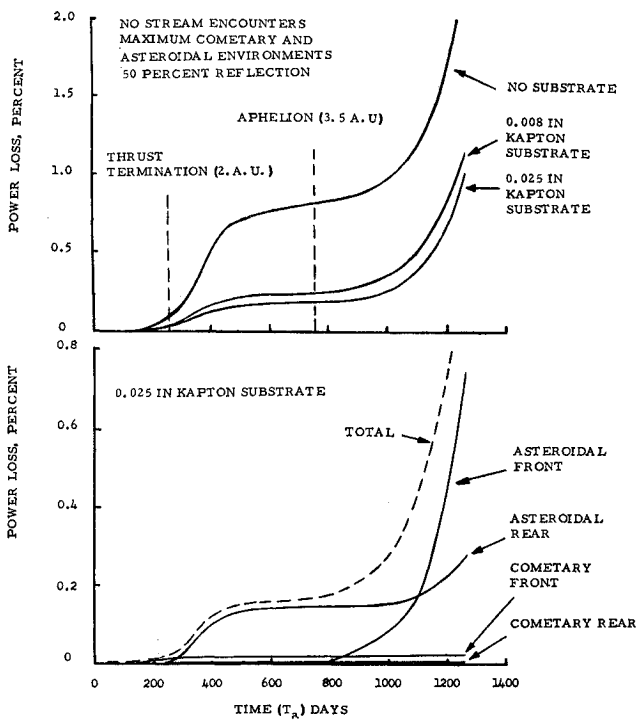

Fig. 4 Power loss during asteroid belt mission.

particles, and cometary stream particles. Recent NASA models[4] describe the flux of the first two by the equation

$$N = 10^{-C_1}V/4m^{C_2} \tag{3}$$

The constants C_1 and C_2 can be obtained from the environment model and will vary with the type of particle and range of mass. The total solar panel front surface area fractured by impacts of particles of mass m to $m + dm$ is

$$dA_{L1} = A_{L1}'dn = [C_2V10^{-C_1}A_{L1}'A_{spe}T_R/4m^{(C_2+1)}]dm \tag{4}$$

Assuming that all particle impacts are separate, the total area fractured by all impacts will be the integral of Eq. (4) over the range of masses to be encountered. Using Eq. (2), the solar panel area that is fractured by meteoroid impacts on the front surface is

$$A_{L1} = 33C_2V^{7/3}10^{-C_1}T_R\alpha^2K^2\rho^{0.2}A_{spe}\int_{m_1}^{m_2}\left[\frac{1}{m^{(C_2+0.2)}}\right]dm \tag{5}$$

For the lower limit, m_1 is assumed to be the mass of the smallest particle that can be held in orbit around the sun, $m_1 = 1 \times 10^{-12}$ g. The upper limit of mass is established so that there is a probability of only 0.001 that a particle of mass m_2 or greater will impact on the area A_{sp} during the time T_R. The probability of one or more impacts of a particle of mass m_2 or greater is given by a Poisson distribution $P_r = NA_{spe}T_R$, and applying Eq. (3)

$$m_2 = [250V10^{-C_1}A_{spe}T_R]^{1/C_2} \tag{6}$$

Rear surface impacts

Meteoroid impacts into the rear of a solar panel require different treatment since the particle will not cause solar cell penetration until it perforates the substrate material or

$$P_{sc} = P - t_3 = K\rho^{1/2}V^{2/3}d_p^{1.2} - t_3$$

Applying the same reasoning used in the front surface analysis, the solar panel area that is fractured by meteoroid impacts on the rear surface is

$$A_{L2} = 19.64\,\alpha^2C_2V10^{-C_1}T_RA_{spe}\Bigg\{1.68K^2\rho^{0.2}V^{4/3}\times$$
$$\int_{m_1}^{m_2}\left[\frac{1}{m^{(C_2+0.2)}}\right]dm - 2.592\,K\rho^{0.1}V^{2/3}t_3\times$$
$$\int_{m_1}^{m_2}\left[\frac{1}{m^{(C_2+0.6)}}\right]dm + t_3^2\int_{m_1}^{m_2}\left[\frac{1}{m^{(C_2+1.0)}}\right]dm\Bigg\} \tag{7}$$

The upper limit of mass was defined as in the front surface analysis. The lower limit was defined as the mass of the smallest particle that would just perforate t_3, which by Eq. (1) is

$$m_1 = (t_3/1.296K\rho^{0.1}V^{2/3})^{2.5} \tag{8}$$

where t_3 is the thickness of a glass substrate. The penetration into a nonglass substrate was taken as[5]

$$P_s = K_s\rho^{1/2}V^{2/3}d_p^{1.1}/H_s^{1/4}\rho_s^{1/6} \tag{9}$$

Applying Eqs. (1) and (9), the effective thickness of nonglass substrate is

$$t_3 = 0.287t_sH_s^{1/4}\rho_s^{1/6} \tag{10}$$

Since the cometary particles are treated as omnidirectional, the effective solar panel area is the panel surface area ($A_{spe} = A_{sp}$). The asteroidal particles are considered to be in circular orbits near the ecliptic plane, resulting in a unidirectional flux. Therefore, the effective panel area for these particles was defined as $A_{spe} = A_{sp}\sin\phi$.

Application to Asteroid Belt Mission

The spacecraft configuration evaluated was one developed under JPL contract,[6] and was based on use of a Mercury Electron Bombardment Ion propulsion system, Fig. 2. The study trajectory was a 1190-day mission through the asteroid belt (Fig. 3) chosen to gather data in this region of the solar system. Due to the large variation in impact velocity and flux throughout the mission, area losses were calculated for small segments of the mission and summed to obtain total area loss. Assuming that the power loss will be 50% of the area loss, the percent power loss was computed for the spacecraft with various substrate thicknesses, Fig. 4. The model of Ref. 7 was applied to estimate the extent of the meteoroid stream hazard. It was found that the number of active zones encountered was very sensitive to departure date. An Oct. 1, 1975 launch would result in one encounter and a Nov. 1, 1975 launch date in no encounters. An intermediate departure date of Oct. 22, 1975 would result in four encounters. The Oct. 1, 1975 launch trajectory would pass through the stream of the comet Schaumasse in fall 1977, with a predicted power less of 2.5%.

Conclusions

1) Providing the meteoroid environment models used define the true upper limit of the sporadic meteoroid population, the solar panel power loss during the 1190-day study mission because of sporadic cometary and asteroidal particles would have an absolute upper limit of 8% based on a 100% fracture zone reflection, and a best estimate upper limit of 4% based on a 50% reflection factor. 2) The addition of a substrate should significantly reduce the above power loss values (Fig. 4), with 0.002-in. thick Kapton or equivalent being helpful, and 0.008-in. providing the maximum benefit. 3) Hypervelocity impact testing of solar cells is recommended for the determination of the effective reflection factor associated with a given solar panel design. The 10^{-6} g glass particles fired by the electrothermal hypervelocity impact guns closely approximate the meteoroid particles predicted to be the main source of solar panel degradation. These test facilities are therefore a logical choice for determination of reflection factors. 4) The power loss values previously noted can be significantly increased if the solar panels are exposed to a cometary stream or streams. Therefore, launch dates should be selected which avoid encounters with the known active shower zones.

References

[1] Bowman, R. L., Mirtich, M. J., and Jack, J. R., "Performance of N/P Silicon and Cadmium Sulfide Solar Cells as Affected by Hypervelocity Particle Impact," TN D-513, March 1969, NASA.

[2] Flaherty, R., "Impact Characteristics in Fused Silica for Various Projectile Velocities," *Journal of Spacecraft and Rockets*, Vol. 8, No. 3, March 1970, pp. 319–324.

[3] McHugh, A. H. and Richardson, A. J., "Hypervelocity Particle Impact Damage to Glass," STR 241, Jan. 1971, Space Div., North American Rockwell, Downey, Calif.

[4] Kessler, D. J., "Meteoroid Environment Model—1970 [Interplanetary and Plantary]," NASA SP-8038, Oct. 1970.

[5] Richardson, A. J. and McHugh, A. H., "Hypervelocity Impact Penetration Equation for Metal by Multiple Regression Analysis," STR 153, March 1966, Space Div., North American Rockwell, Downey, Calif.

[6] Richardson, E. H., "Solar Electric Propulsion Asteroid Belt Mission Study Final Report," SD 70-21-2, Jan. 1970, Space Div., North American Rockwell, Downey, Calif.

[7] Dycus, R. D. and Richardson, A. J., "A Meteoroid Stream Model for Evaluation of the Stream Hazard to Interplanetary Flight," *Journal of Spacecraft and Rockets*, Vol. 7, No. 9, Sept. 1969, pp. 1070–1072.

Chemical Nonequilibrium Boundary-Layer Effects on a Simulated Space Shuttle Configuration during Re-Entry

JOHN C. ADAMS JR.*
ARO Inc., Arnold Air Force Station, Tenn.

FUTURE space shuttle missions dictate lifting entry into the Earth's atmosphere under conditions which place stringent requirements on the vehicle's thermal protection system (TPS). General surveys of the severe heating environment during space shuttle re-entry and the current thinking toward solution of these problems have been given in recent articles by Faget[1] and Lecat.[2] The shuttle vehicle will re-enter at higher altitudes and lower velocities than did previous vehicles, which means that chemical nonequilibrium phenomena in the shock layer will become of increasing importance. Because currently proposed shuttle vehicles are long (~100 ft), nonequilibrium relaxation effects must be considered in estimates of nonequilibrium heating rates to be encountered under high altitude re-entry conditions. The present Note reports an investigation into chemical nonequilibrium boundary-layer effects on a simulated space shuttle configuration (a 20° half-angle sphere-cone having a nose radius of 1.0 ft) at zero angle of attack under altitude-velocity conditions of 200,000 ft and 16,000 fps in the Earth's atmosphere. Since a metallic reradiation heat shield will probably be used for the shuttle TPS, a constant wall temperature of 2000°R is assumed. Total body length is taken to be 100.0 ft. Although the sphere-cone geometry at zero angle of attack is not an accurate representation of current shuttle concepts, the results reported herein should be representative of the nonequilibrium effects to be expected.

Analysis

The present investigation makes use of the chemical nonequilibrium laminar boundary-layer analysis reported by Adams et al.[3] in conjunction with an inviscid streamline absorption technique similar to that used by Kaplan.[4] The following assumptions and guidelines are followed in the boundary-layer analysis: 1) The boundary layer is laminar. 2) The basic gas model is a multicomponent mixture of chemically reacting perfect gases made up of N, O, N_2, O_2, NO, NO^+, and e^-. The gas is in vibrational equilibrium but in chemical nonequilibrium as controlled by the 11-chemical-reaction model used by Blottner[5] with the reaction rates of Bortner.[6] 3) Multicomponent diffusion between species is allowed throughout the viscous region. For the ionized species, ambipolar diffusion is employed; thermal diffusion is neglected for all species. Enthalpies, specific heats, and binary diffusion coefficients for the individual species are taken from Blottner,[5] whereas viscosity and thermal conductivity for the mixture are obtained from Wilke's formula using individual species properties from Blottner.[5] 4) Effects of wall surface conditions are considered by examining both noncatalytic and fully catalytic walls following Lenard.[7] 5) Radiative phenomena in the boundary layer (emission and absorption) are not

Received December 14, 1970; revision received January 29, 1971. This work was sponsored by the Arnold Engineering Development Center (AEDC), Air Force Systems Command, U. S. Air Force under Contract F40600-71-C-0002 with ARO Inc., Contract Operator, AEDC. Further reproduction is authorized to satisfy needs of the U.S. Government.

* Supervisor, Special Studies Group, Aerodynamics Section, Hypervelocity Branch, Aerophysics Division, von Kármán Gas Dynamics Facility. Member AIAA.